# VI

Publication VI

Teemu Ojanen and Janne Salo, *Possible scheme for on-chip element for squeezed microwave generation*, Physical Review B **75**, 184508 (2007).



http://link.aps.org/abstract/prb/v75/p184508

# Possible scheme for on-chip element for squeezed microwave generation

T. Ojanen[1,*] and J. Salo[2]
[1]*Low Temperature Laboratory, Helsinki University of Technology, P.O. Box 2200, FIN-02015 HUT, Finland*
[2]*Laboratory of Physics, Helsinki University of Technology, P.O. Box 4100, FIN-02015 HUT, Finland*
(Received 13 September 2006; revised manuscript received 2 March 2007; published 8 May 2007)

We propose a scheme to generate squeezed microwave radiation into a transmission line using a simple on-chip element. Instead of the more commonly used quadratic $i(\hat{a}^{\dagger 2}-\hat{a}^2)$ Hamiltonian, the element is based on parametric resonance drive, $(\hat{a}^\dagger+\hat{a})^2\cos 2\omega_0 t$, which can approximately be realized using an ac magnetic flux on a superconducting quantum interference device (SQUID) loop. The dissipation arising from the coupling to the transmission line is also included in the dynamics, and it is, in fact, essential for the formation of the (periodically) steady squeezed SQUID state. The spectral properties of the radiation are calculated and they differ somewhat from the conventional squeezing. With a proper choice of parameters, the quadrature noise can be suppressed below its ground-state value, a direct evidence of reduction of the quantum fluctuations. We also present a measurement setup for direct verification of the phenomenon. The squeezing element provides a tool for quantum noise engineering and its simplicity allows a flexible integration into more complex quantum devices.

DOI: 10.1103/PhysRevB.75.184508 PACS number(s): 85.25.Dq, 74.40.+k, 85.25.Cp

## I. INTRODUCTION

Squeezing of quantum fluctuations has first been studied and experimentally verified in quantum optics, where the components of quantized electric field served as the squeezed observables.[1] Since then, the phenomenon has been observed in superconducting circuits,[2,3] and more recently, there has been promising effort to realize the squeezing in nanomechanical structures[4,5] and in circuit cavity QED.[6] Experimentally, the squeezing of the quantum fluctuations has been demonstrated in microwave frequencies by constructing a Josephson parametric amplifier,[3] with a 40% reduction of the vacuum noise.

We consider a setup that allows squeezing of the quantum state of a mesoscopic superconducting quantum interference device (SQUID) element and, subsequently, generation of squeezed microwave radiation. We choose to employ parametric instability in a harmonic regime,[8] a procedure known to create squeezing in various different systems,[9] rather than rapid decrease of an external magnetic flux theoretically studied in Ref. 7. It can be realized with an elementary flux control in an rf SQUID. In the parameter range considered, the system can be thought as an electromagnetic counterpart of nanomechanical resonators with similar application prospects.[5] With little or no dissipation, the magnitude of the squeezing grows exponentially and rotates between the charge and the magnetic flux.[10] A strong dissipation, here realized by coupling to a transmission line, compensates the resonant drive and leads to a rotating quasistationary state in which uncertainties of SQUID observables periodically go below their ground-state values. A significant advantage of the proposed squeezing scheme is that the harmonic drive maintains coherence even in the presence of strong dissipation. Hence, the creation of squeezed states is robust against environmental effects and does not require samples of particularly high quality. We calculate the expectation values of observables and noise spectrum of the radiation in the transmission line, and also propose a measurement scheme for experimental verification of the quantum squeezing.

## II. SQUEEZING BY PARAMETRIC RESONANCE

In the parametric resonance,[11] periodic time-dependent perturbation can lead to large effects, which are most significant when the period of the perturbation is twice the resonance frequency,

$$H=\frac{p^2}{2m}+\frac{m}{2}(\omega_0^2+A\cos 2\omega_0 t)x^2, \tag{1}$$

where the time-dependent part can be treated as a perturbation, $|A|\ll\omega_0^2$. Driven in resonance, the energy of the system grows exponentially in time; additionally, starting the resonant driving from the ground state of a quantum-mechanical harmonic oscillator results in a rapid squeezing of uncertainties of rotating conjugate observables (see Sec. V below).

This mechanism can be realized using a flux-controlled rf SQUID loop described in Fig. 1. The Hamiltonian for the system can be written as

$$H=\frac{\hat{Q}^2}{2C}+\frac{\hat{\phi}^2}{2L_S}-E_J\cos[\Phi(t)2e/\hbar]\cos(\hat{\phi}2e/\hbar), \tag{2}$$

where $C$ is the capacitance of the junctions, $L_S$ is the self-inductance of the loop, and $\Phi(t)$ is the flux bias externally applied through the control loop.[12] The quantities $\hat{Q}$ and $\hat{\phi}$ are the canonical variables corresponding to the charge in the junctions and the magnetic flux through the loop, and they satisfy the commutation relation $[\hat{\phi},\hat{Q}]=i\hbar$. Thus, the magnetic flux $\hat{\phi}$ plays the role of the position coordinate and the charge $\hat{Q}$ corresponds to the momentum in the standard one-particle quantum mechanics.

The flux value corresponding to the oscillator length of the harmonic part of Eq. (2) is $\phi_0=\sqrt{\hbar Z_0}$, where $Z_0=\sqrt{L_S/C}$.

We treat the Josephson term as a perturbation and there-

 

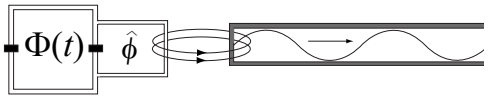


FIG. 1. Resonantly driven SQUID loop inductively coupled to a transmission line. The black bars represent Josephson junctions and the physical quantities $\hat{\phi}$ and $\hat{Q}$ correspond to the magnetic flux through the right loop and the charge at the junctions. The (classical) flux $\Phi(t) \propto \sin(\omega_0 t)$ through the larger loop is controlled by an external magnetic field.

fore consider the parameter range $L_S \ll L_J$, where the Josephson inductance is $L_J = \hbar^2/4e^2E_J$. If the quadratic potential is strong, the flux particle is restricted to the linear regime of the SQUID, and only the lowest two terms of the expansion $\cos(\hat{\phi}2e/\hbar) = 1 - \hat{\phi}^2 e^2/\hbar^2 + 2\hat{\phi}^4 e^4/3\hbar^4 + \cdots$ are retained. Supposing that the condition for the validity of the approximation $\phi_0 < \Phi_0 = h/2e$ is satisfied, the Hamiltonian (2) takes the form

$$H \approx \frac{\hat{Q}^2}{2C} + \frac{C\omega^2(t)}{2}\hat{\phi}^2, \tag{3}$$

where

$$\omega^2(t) = \omega_0^2\left\{1 + \frac{L_S}{L_J}\cos[\Phi(t)2e/\hbar]\right\}, \tag{4}$$

with $\omega_0^2 = (L_S C)^{-1}$. The small term constant in $\hat{\phi}$ resulting from the cosine expansion has been dropped from Eq. (3). Now we have established a connection between Eqs. (1) and (3) provided that the external magnetic flux is modulated according to $\Phi(t) = \hbar\omega_0 t/e$.

The linearly increasing magnetic flux is, in practice, inconvenient since the magnetic field should be restricted to the control loop, and it is difficult to isolate at high field values. In addition, ac fields are obtained and manipulated more naturally. We would like to implement the parametric resonance by replacing the linearly increasing flux with an ac flux $\Phi(t) = \beta\Phi_0 \sin(\omega_0 t)$. In fact, this can be achieved remarkably accurately. The cosine of sine can be expanded in terms of the Bessel functions as $\cos[\alpha \sin(x)] = J_0(\alpha) + 2\Sigma_n J_{2n}(\alpha)\cos(2nx)$. This relation suggests that $\alpha$ should be chosen so that $2J_2(\alpha)$ is close to unity to realize $\cos(2x) \approx \cos[\alpha \sin(x)]$ (the other terms in the expansion are small and, importantly, nonresonant). The maximum of $J_2(\alpha)$ is 0.49, which is achieved at $\alpha \approx 3.05$. Since $J_2(\alpha)$ changes slowly around its maximum, we choose $\alpha = 3$. We introduce an ac field flux

$$\Phi(t) = (3/2\pi)\Phi_0 \sin(\omega_0 t) \tag{5}$$

to produce the required resonance term in the Hamiltonian. Despite the mathematical arguments, the previous consideration serves only as a motivation. Ultimately, the validity of the approximation is proven by the resulting dynamics which coincides accurately with the exact results (for example, see Fig. 1 of Ref. 10). In all the calculations presented in this paper, the ac-approximation results coincide with the exact cosine results within a few percent of the relevant scale. Numerical solutions indicate that the best agreement is achieved around $\alpha = 3$ and verify, as expected, that $\alpha$ could be chosen from the interval $2.9 \leqslant \alpha \leqslant 3.1$ without affecting the validity of the approximation significantly. In conclusion, to implement the parametric resonance using ac driving, the magnetic flux should be modulated at the resonance frequency in such a way that its amplitude is roughly a half of the flux quantum. For realistic SQUID, parameter satisfying the above stated requirements can be given order of magnitude estimates $C = 1$ pF, $L_S = 10$ nH, $\omega_0/2\pi = 5$ GHz, $Z_0 = 320\ \Omega$, and $L_J = 100$ nH.

For later purposes, it is convenient to introduce the second-quantized bosonic creation and annihilation operators $\hat{a}$ and $\hat{a}^\dagger$ in the photon number Fock space. The SQUID observables may be then written as

$$\hat{\phi} = \sqrt{\hbar Z_0/2}(\hat{a} + \hat{a}^\dagger) = \sqrt{\hbar Z_0}\hat{\phi}',$$

$$\hat{Q} = i\sqrt{\hbar/2Z_0}(\hat{a}^\dagger - \hat{a}) = \sqrt{\hbar/Z_0}\hat{Q}'. \tag{6}$$

Here, $\hat{\phi}' = \frac{1}{\sqrt{2}}(\hat{a}^\dagger + \hat{a})$ and $\hat{Q}' = \frac{i}{\sqrt{2}}(\hat{a}^\dagger - \hat{a})$ are scaled phase and charge operators, and they satisfy the minimum uncertainty condition $\Delta\phi'\Delta Q' \geqslant 1/2$.

In this notation, the Hamiltonian in Eq. (3) is transformed to

$$\hat{H} = \hbar\omega_0\left(\hat{a}^\dagger\hat{a} + \frac{1}{2}\right) + B\cos(2\omega_0 t)(\hat{a} + \hat{a}^\dagger)^2, \tag{7}$$

where $B = \hbar\omega_0 L_S/4L_J$. Corrections to the higher orders in Eq. (7) due to the Josephson coupling are $D\cos(2\omega_0 t)(\hat{a} + \hat{a}^\dagger)^4$, where the ratio $D/B \propto (\phi_0/\Phi_0)^2$ becomes small in the considered parameter range $\phi_0 \ll \Phi_0$. In addition to being small, the higher-order terms, in contrast to the quadratic one, are not parametrically resonant and their effects are suppressed.

## III. COUPLING THE SQUID TO A TRANSMISSION LINE

In this section, we introduce a measuring scheme in which the SQUID is coupled to a transmission line (TL) that serves as a waveguide carrying away the radiation from the system. It also plays a role of a generic measurement device which causes a Markovian back action to the SQUID system. Additionally, the TL provides a practical theoretical model for studying the environmental effects to the squeezing.

The transmission line acts as a one-dimensional electromagnetic field inductively coupled to the quantized flux $\hat{\phi}$ of the SQUID loop. Then, the free Hamiltonian of the line is

$$H_{\mathrm{TL}} = \sum_m \hbar\omega_m(\hat{c}_m^\dagger\hat{c}_m + 1/2), \tag{8}$$

whereas the coupling is given by

$$H_{\mathrm{int}} = M\frac{\phi}{L_S}\sum_k i\sqrt{\frac{\hbar\omega_k}{Ll}}(-\hat{c}_k + \hat{c}_k^\dagger). \tag{9}$$

Here, $M$ is the mutual inductance between the loop and the field modes in the transmission line. $\hat{c}_k$ and $\hat{c}_k^\dagger$ are the bosonic

annihilation and creation operators of the electromagnetic field modes and

$$\hat{V}(x_0,t) = \sum_k \sqrt{\frac{\hbar\omega_k}{Lc}} \cos\left(\frac{k\pi}{L}x_0\right)[\hat{c}_k(t) + \hat{c}_k^\dagger(t)] \quad (10)$$

is the voltage operator in the transmission line at distance $x_0$ from the SQUID loop.[13]

Assuming that the excited states of the SQUID are not thermally populated ($\hbar\omega_0 > k_B T$) and that no signal arrives from the transmission line, the dominating environmental effect is spontaneous emission into TL. With the parameter values given above, this is achieved for $T \approx 100$ mK. Due to the coupling to the transmission line, the SQUID itself is an open quantum system and is consequently described by a density operator obeying the Lindblad-type master equation[14]

$$\partial_t \rho = -\frac{i}{\hbar}[H,\rho] + \kappa(2\hat{a}\rho\hat{a}^\dagger - \hat{a}^\dagger\hat{a}\rho - \rho\hat{a}^\dagger\hat{a}), \quad (11)$$

where the first term is responsible for the Hamiltonian evolution by the operator (7) and the second term describes the spontaneous emission into the TL. The coefficient $\kappa$ is related to the quality factor of the circuit by $\kappa = \omega_0/Q$, where the $Q$ factor can be as high as $10^3$–$10^4$ in the case of a free SQUID. Coupling to the TL should decrease $Q$ significantly in order to guarantee an efficient measurement of the SQUID. The value of $\kappa$ can be calculated as $\kappa/\omega_0 = (M/L_S)^2 Z_0/Z_{\mathrm{TL}}$, where $Z_{\mathrm{TL}} = \sqrt{l/c}$. For realistic values $M/L_S = 0.1$ and $Z_{\mathrm{TL}} = 50\ \Omega$ and the rest SQUID parameters taking previously stated values, the fraction becomes $\kappa/\omega_0 \approx 0.06$ which corresponds to $Q \approx 20$. A free SQUID can have a $Q$ value of order of 100, corresponding to a coherence time of 20 ns, without significantly affecting to the radiation; thus, only modest coherence properties are required. The disadvantage of decreased $Q$ is the increased decoherence, hostile to the squeezing process.

On the other hand, the SQUID radiates into the transmission line, and we can represent the voltage operator as

$$\hat{V}(x,t) = \hat{V}_0(x,t) + \frac{M\omega_0}{\pi L_S}\hat{\phi}(t - x/v), \quad (12)$$

where $\hat{V}_0(x,t)$ is the voltage operator in the absence of the SQUID loop, and the second term is proportional to the retarded SQUID field. In radiation problems, observables are typically of this form.[14] In derivation of Eq. (12), we have assumed that the level separation in the TL is much smaller than $\omega_0$, so the TL will act as a waveguide and not as a resonator. The voltage radiated into the transmission line is thus proportional to the phase operator $\hat{\phi}$ of the SQUID, and we may, for the time being, concentrate only on the dynamics of the latter.

## IV. SQUID DYNAMICS UNDER DISSIPATION

The master equation (11) allows, in principle, one to solve the entire quantum state of the SQUID system, but this is not always necessary. Rather, SQUID observables and the properties of the field radiated into the transmission line are sufficiently described by the one-time expectation value of the voltage operator and corresponding two-time correlation functions that determine the noise spectrum.

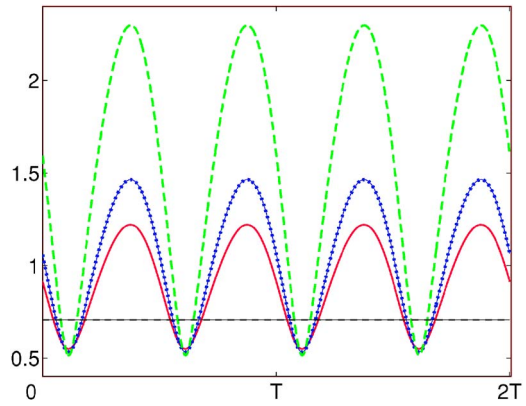


FIG. 2. (Color online) Uncertainty $\Delta\phi'$ of the bounded periodic solutions $\kappa = 1.5B$ (solid line), $\kappa = 1.3B$ (dotted line), and $\kappa = 1.1B$ (dashed line). The horizontal dashed line marks the ground-state value of $\Delta\phi'$. The lower envelope of the oscillation depicts the uncertainty of the reduced quadrature, while the higher envelope corresponds to the increased quadrature of the rotating state. The minimum of the squeezing in the periodic solutions approaches to lower bound of about 0.75 times the ground-state value.

The expectation values of $\hat{a}$, $\hat{a}^\dagger$, $\hat{a}^2$, $\hat{a}^{\dagger 2}$, and $\hat{a}^\dagger\hat{a}$ can be solved from the coupled set of differential equations of the form $\partial_t\langle\hat{a}\rangle = \mathrm{Tr}[\hat{a}\partial_t\rho]$, etc.[10] For a strong drive, $B > \kappa$, the expectation values grow increasingly in time, while for $\kappa > B$, the dissipation eventually compensates the resonant drive and the solutions are periodic and bounded. We then find an accurate analytical form for the periodic solution by expanding the expectation values $\langle\hat{a}^\dagger\hat{a}\rangle$, $\langle\hat{a}^2\rangle$, and $\langle\hat{a}^{\dagger 2}\rangle$ to a Fourier series as $\langle\hat{a}^\dagger\hat{a}\rangle = \Sigma_{-\infty}^{\infty}\alpha_n \exp(2in\omega_0 t)$ and similarly for other combinations. Truncating the series to the fourth order, the lowest Fourier coefficients can be found by solving the linear system. In the limit $\kappa \to B+0$, the lower limit of the periodic squeezing is about 0.75 times the vacuum value of $\Delta\phi'$ and $\Delta Q'$ (see Fig. 2).

We illustrate the squeezing using the Wigner function

$$\rho_W(x',p') = (2\pi)^{-1}\int_{-\infty}^{\infty}\left\langle x' - \frac{1}{2}y\middle|\rho\middle|x' + \frac{1}{2}y\right\rangle e^{ip'y}dy, \quad (13)$$

which is one of the quantum-mechanical analogs to the phase-space probability distribution. Even though it is not a genuine two-dimensional probability distribution, it correctly produces the one-dimensional marginal distributions in arbitrary directions in the phase space $(x',p')$ and can therefore be used directly to visualize the uncertainties of observables.

The circularly symmetric ground state of the SQUID is distorted to an ellipse by squeezing (see Fig. 3). For ideal squeezed states, the principal axes of elliptical contour lines are inversely proportional reflecting the minimum uncertainty property. The effect of the dissipation on squeezed states is twofold: On one hand, the distribution is broadened,

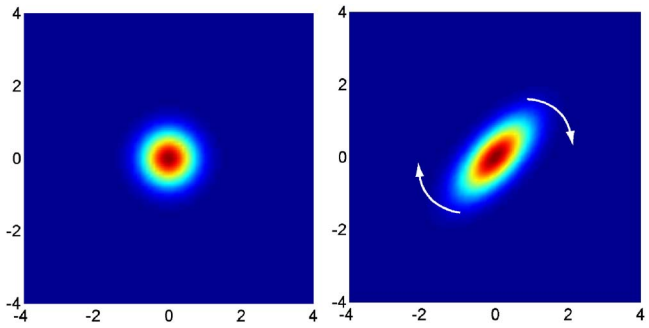

FIG. 3. (Color online) Wigner function of the ground state (left) and the periodic squeezed state $\kappa=1.5B$ (right) in the $(\phi',Q')$ plane. The squeezed state rotates clockwise as indicated by the arrows. The ellipse makes $2\pi$ rotation in time $T=2\pi/\omega_0$.

which, most importantly, increases the uncertainty of the narrower quadrature and the state no longer is a proper minimum uncertainty state. On the other hand, spontaneous emission of individual photons into the TL also populates the states of odd number of excitations, which are entirely absent in the ideal squeezed states of minimum uncertainty.

In order to find the spectral properties of the signal radiated into the TL, we also need to evaluate two-time correlation functions, such as $\langle\hat{a}^\dagger(t_2)\hat{a}(t_1)\rangle$. According to the quantum regression formula,[14] the function pair $\langle\hat{A}(t)\hat{a}(t')\rangle$ and $\langle\hat{A}(t)\hat{a}^\dagger(t')\rangle$ obeys the same differential equations as $\langle\hat{a}(t')\rangle$ and $\langle\hat{a}^\dagger(t')\rangle$ for an arbitrary operator $\hat{A}(t)$. Choosing $\hat{A}(t)=\hat{a}^{(\dagger)}(t)$, arbitrary second-order correlators can be found numerically in the entire time domain.

## V. SPECTRUM OF PARAMETRIC RESONANCE AND SQUEEZING

In order to describe the signal carried by the transmission line, we briefly consider a spectral analyzer based on a two-level system[13] with an energy splitting $\Omega=\Delta E$. The probability of observing the analyzer system in its states is proportional to

$$\int_0^t\int_0^t\langle A(t_1)A(t_2)\rangle e^{-i\omega(t_2-t_1)}dt_1dt_2 \tag{14}$$

at $\omega=\pm\Omega$, where $A$ is the operator of the studied noise source that couples to the analyzer two-level system. Now the SQUID radiation is periodic rather than steady state, and the detector rate is proportional to the time-averaged noise power

$$S_A(\omega)=\int_{-\infty}^{\infty}\frac{1}{T}\int_0^T\langle A(\tau+t')A(t')\rangle e^{i\omega\tau}dt'd\tau, \tag{15}$$

where $T$ is the period of the evolution. Expression (15) generalizes the standard steady-state solution in the sense that so defined spectrum is positive definite and gives excitation probabilities of the analyzer system in the long-time limit $t\gg T=2\pi/\omega_0$. Based on Eq. (12), the spectral properties of $\hat{V}(x,t)$ are directly related to spectral properties of $\hat{\phi}$ and the free voltage operator $\hat{V}_0$, and we therefore evaluate the $\hat{\phi}$ noise and, at the end of this section, discuss parameters relevant to the TL output noise.

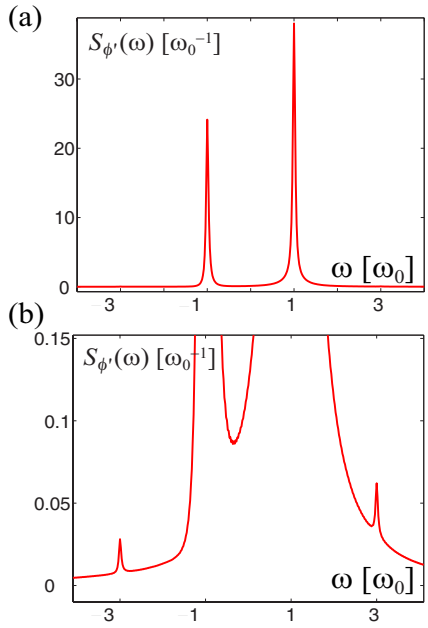


FIG. 4. (Color online) (a) Time-averaged noise spectrum $S_{\phi'}(\omega)$ of the periodic squeezed state $\kappa=0.15\omega_0=1.25B$. The spectrum has resonances at frequencies $\pm\omega_0$. (b) The fine structure of spectrum (a) reveals the weak resonance peaks at $\pm3\omega_0$.

The $2\omega_0$ resonant drive produces peaks in the $\hat{\phi}$ spectrum (15) at frequencies $\pm(2n+1)\omega_0$ of which the $\pm\omega_0$ are by far the strongest with relative thermal population (see Fig. 4). The higher harmonic peaks are very weak. From the time-averaged observables, it is difficult to detect the squeezing directly. This can be understood by considering the Wigner function: the fast rotation of the elliptic figure in Fig. 3 averages out to a circular shape, the diameter of which corresponds to the broader quadrature and in which no squeezing is present; the overall broadening compared to the ground state only appears as an equilibrium state at a finite temperature.

### A. Spectrum of rotating operators

A detailed detection of squeezing can be performed using a phase-sensitive measurement. For that purpose, we define the rotating-frame operators as $\hat{b}(t)=\exp(i\omega_0t+i\theta)\hat{a}(t)$ and $\hat{b}^\dagger(t)=\exp(-i\omega_0t-i\theta)\hat{a}^\dagger(t)$. The rotating SQUID observables are defined analogously as $\hat{\phi}_r'=[\hat{b}(t)+\hat{b}^\dagger(t)]/\sqrt{2}$ and $\hat{Q}_r'=i[\hat{b}^\dagger(t)-\hat{b}(t)]/\sqrt{2}$, and rotations of $\hat{b}(t)$ and $\hat{b}^\dagger(t)$ compensate the natural rotation of the harmonic creation and annihilation operators. In the new operators, the orientation of the squeezing is (nearly) static and is determined by the angle $\theta$; the Wigner functions in Fig. 3 appear frozen in time. Only a tiny time-dependent deformation resulting from the drive remains.

The noise varies periodically as a function of $\theta$ as the orientation of the squeezing is rotated (see Fig. 5). For a

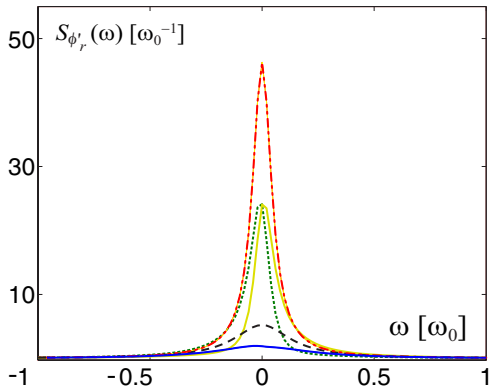


FIG. 5. (Color online) Noise spectrum $S_{\phi'_r}(\omega)$ of the squeezed state $\kappa=0.15\omega_0=1.5B$ in the rotating operators. The resonance peaks are now moved to the origin. The blue solid curve shows the spectrum of the minimum-noise quadrature, and the other curves (green dotted, red dash-dotted, and yellow solid) correspond to the noises of the quadratures rotated with $\pi/4$, $\pi/2$, and $3\pi/4$, respectively, with respect to the quadrature of the minimal noise. The black dashed curve represents the ground-state noise. Evidence of squeezing is obtained whenever the noise of some quadrature lies below the ground-state level.

finite range of $\theta$, the SQUID noise of the $\hat{\phi}'_r$ observable goes below its ground-state value, which is a direct evidence of reduction of the quantum fluctuations. For the parameters of Fig. 5, the ground-state noise at zero frequency is approximately 2.5 times higher than the minimum noise corresponding to $\theta=0$. The noise curves of squeezed states are slightly asymmetric with respect to the half axes of the ellipse in Fig. 3, a consequence for the fact that the parametric drive in the presence of a dissipation does not exactly produce ideal squeezed state. In Sec. VI below, we will shortly discuss how to measure the rotating spectrum.

### B. Transmission line output

The TL voltage observable is the sum of the free-line voltage operator and the retarded SQUID radiation contribution [see Eq. (12)]. Since the two are uncorrelated, the voltage noise spectrum is given by $S_V(\omega)=S_V^0(\omega)+g^2S_{\phi'}(\omega)$, where $S_V^0(\omega)$ is the vacuum noise of the TL and the coupling constant $g$ depends on the material parameters and can be deduced from Eq. (12):

$$g=\frac{M\omega_0}{L_S}\sqrt{\hbar Z_0}, \tag{16}$$

where $Z_0=\sqrt{L_S/C}$ [$S_{\phi'}(\omega)$ is the noise in the dimensionless flux variable]. For the phenomenon to be measurable, the vacuum noise of the TL should not overwhelm the SQUID noise. From Eq. (16) and the results shown in Fig. 5, we can estimate the order of magnitude as $g^2S_{\phi'_r}(\omega=0)\approx(2-50)(M/L_S)^2\hbar\omega_0Z_0$, where the smaller value corresponds to the blue curve and the greater value to the red curve. Although the noise peak is mathematically shifted to zero in the rotating spectrum, the physical SQUID signal is still peaked around $\omega_0$ and should be compared to the free TL vacuum

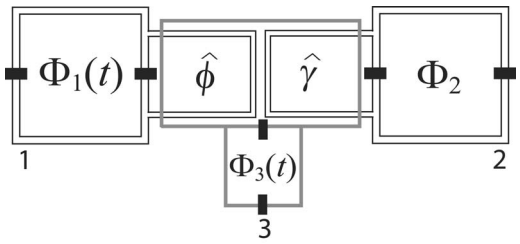


FIG. 6. Schematic circuit for measuring the squeezed spectrum. System 1 on the left is the squeezed SQUID element and system 2 on the right is a flux qubit. The gray loop 3 in the middle mediates the harmonically varying interaction when the flux $\Phi_3(t)$ is modulated with an ac magnetic field. Dissipation mechanism of the squeezed SQUID element is not represented in the figure.

noise at frequency $\omega_0$, which at low temperatures is $S_V^0(\omega_0)=\hbar\omega_0Z_{\mathrm{TL}}$. Then, the relative effect is of order $g^2S_{\phi'_r}(\omega=0)/S_V^0(\omega_0)=(2-50)(M/L_S)^2Z_0/Z_{\mathrm{TL}}=(2-50)\kappa/\omega_0$. Taking $\kappa/\omega_0=0.15$, as in Fig. 5, the fraction becomes $g^2S_{\phi'_r}(0)/S_V^0(\omega_0)=0.3-7.5$, depending on the direction of squeezing, suggesting that the SQUID noise has a significant effect on the TL output radiation in favorable conditions. In the next section, we give an example of how the rotating spectrum can be measured.

## VI. MEASUREMENT OF SQUEEZING BY A QUBIT

In this section we briefly discuss how the squeezed spectrum can be accessed directly. We assume that the SQUID flux $\hat{\phi}'$ is coupled to a two-state quantum system (qubit) according to a total Hamiltonian,

$$H=H_{\mathrm{SQUID}}+H_{\mathrm{env}}+g_c\hat{\phi}'\cos(\omega_0t)\sigma_z+\frac{B_z}{2}\sigma_z, \tag{17}$$

in which the SQUID flux $\hat{\phi}'$ couples time dependently to the qubit through $\sigma_z$ operator. Here, $B_z$ is the qubit energy splitting and $g_c$ is the coupling strength. The terms $H_{\mathrm{SQUID}}$ and $H_{\mathrm{env}}$ describe the SQUID and its dissipative environment, leading to dynamics studied previously. The time-dependent SQUID-qubit coupling is essential for compensating effects of rotating squeezing angle. If the systems are weakly coupled, the dephasing time of the qubit can be obtained perturbatively as $1/T_2=\frac{2g_c^2}{\hbar^2}S_{\phi'_r}(0)$, where $S_{\phi'_r}(0)$ is the spectrum of rotating SQUID operators at zero frequency. As can be seen from Fig. 5, this quantity depends strongly on the squeezing angle. Thus, by measuring the dephasing time of the qubit, one can directly verify the squeezing of the spectrum. The squeezing angle $\theta$ can be varied by detuning the relative phase of parametric driving and SQUID-qubit coupling term.

The measurement setup described above could be realized by the circuit depicted in Fig. 6. For simplicity, it consists of three similar circuit elements operated in different parameter regimes. The original squeezed SQUID element is coupled to a Josephson flux qubit by a third loop. All three circuits are described by the Hamiltonian of type (2) with different relative magnitudes of parameters. System 1 is the original

SQUID circuit studied so far, system 2 is a flux qubit, and system 3 is the mediating circuit responsible for the harmonic modulation of the mutual interaction between systems 1 and 2. In system 2, the Josephson energy is large enough to produce well-defined double well potential when the external flux bias is close to $\Phi_0/2$ through the loop associated by a total flux $\hat{\gamma}$.[12] In system 3, the Josephson energy is assumed to be dominant, the other terms being negligible. The effective Hamiltonian for the whole system is

$$H = H_1 + H_2 + H_3, \tag{18}$$

where $H_1$ describes the squeezed element and its environment, $H_2$ can be expressed in the basis of the two flux states as $H_2 = \frac{B_z}{2}\sigma_z + \frac{B_x}{2}\sigma_x$, and $H_3 = -E_{J3}\cos[\Phi_2(t)2e/\hbar]\cos[(\hat{\phi} + \hat{\gamma})2e/\hbar]$ introduces the interaction between the first two loops. Parameters $B_z$ and $B_x$ can be tuned by external magnetic fields through loops $\Phi_2$ and $\hat{\gamma}$.

Supposing that the expectation value of flux $\hat{\phi}+\hat{\gamma}$ is well localized and small compared to $\Phi_0$, the second cosine in $H_3$ can be expanded to the second order (flux can be always made small by diminishing the middle loop and allowing only fraction of $\hat{\phi}+\hat{\gamma}$ through it). In addition, applying previously employed trick of modulating the flux as $\Phi_3(t) = (3/2\pi)\Phi_0 \sin(\omega_0 t/2)$, the effective Hamiltonian becomes $H_3 = \frac{2e^2 E_{J3}}{\hbar^2}\cos(\omega_0 t)(\hat{\phi}^2 + \hat{\gamma}^2 + 2\hat{\phi}\hat{\gamma})$. The weak nonresonant quadratic terms $\hat{\phi}^2$ and $\hat{\gamma}^2$ do not produce finite long-time effects and can be neglected. Thus, the effective SQUID-qubit interaction becomes $H_3 \approx H_{\mathrm{int}} = \frac{4e^2 E_{J3}}{\hbar^2}\cos(\omega_0 t)\hat{\phi}\hat{\gamma}$. Writing the qubit flux operator in the two-state approximation as $\hat{\gamma} = \frac{\gamma}{2}\sigma_z$ ($\gamma$ being the flux separation of states) and supposing that the tunneling between the two flux states of the qubit is suppressed $B_x = 0$, we recover a Hamiltonian of the form (17) with $g_c = \frac{\phi_0 \gamma}{\Phi_0^2} E_{J3}$.

If needed, the coupling strength $g_c$ can be reduced by allowing only a fraction of flux $\hat{\phi}+\hat{\gamma}$ through the middle loop. The SQUID-qubit interaction can be turned off by setting $\Phi_2(t) = \Phi_0/4$. Measuring the dephasing time of the qubit in the absence of the SQUID-qubit interaction and then switching it on at different times, one should see the effects of SQUID noise in various squeezing angles. The squeezed noise can also be measured by other flux-sensitive devices[15] by introducing a harmonically modulated interaction.

## VII. CONCLUSIONS

The parametric harmonic driving creates rotating squeezed quantum states in the SQUID ring. In the presence of a strong damping, the magnitude of the squeezing is stationary. The minimum uncertainty in the flux and charge go below the ground-state value periodically. The phenomenon enables a quantum noise engineering which plays an increasingly important role in the quantum measurement theory as well as in the design of practical quantum devices. Squeezed mechanical oscillators could be used, in principle, as ultrasensitive measurement devices for detecting weak classical forces.[5,16] The squeezed SQUID element could be, analogously, used for measuring weak magnetic fields.

The experimental creation of squeezed quantum states in a SQUID by a parametric driving is feasible with the current experimental methods. We have calculated the relevant noise properties of the periodic squeezed state. By introducing a coupling to the transmission line, we have analyzed the fully quantum-mechanical emission spectrum of the SQUID and discussed briefly the conditions of an experimental verification of the phenomenon.

## ACKNOWLEDGMENT

The authors would like to thank Jukka Pekola for valuable discussions and advice.

*Corresponding author. Electronic address: teemuo@boojum.hut.fi

[1] R. Loudon and P. L. Knight, J. Mod. Opt. **34**, 709 (1987).
[2] B. Yurke, P. G. Kaminsky, R. E. Miller, E. A. Whittaker, A. D. Smith, A. H. Silver, and R. W. Simon, Phys. Rev. Lett. **60**, 764 (1988).
[3] B. Yurke, L. R. Corruccini, P. G. Kaminsky, L. W. Rupp, A. D. Smith, A. H. Silver, R. W. Simon, and E. A. Whittaker, Phys. Rev. A **39**, 2519 (1989).
[4] M. P. Blencowe and M. N. Wybourne, Physica B **280**, 555 (2000).
[5] R. Ruskov, K. Schwab, and A. N. Korotkov, Phys. Rev. B **71**, 235407 (2005).
[6] K. Moon and S. M. Girvin, Phys. Rev. Lett. **95**, 140504 (2005).
[7] M. J. Everitt, T. D. Clark, P. B. Stiffell, A. Vourdas, J. F. Ralph, R. J. Prance, and H. Prance, Phys. Rev. A **69**, 043804 (2004).
[8] L. S. Brown and L. J. Carson, Phys. Rev. A **20**, 2486 (1979).
[9] I. Averbukh, B. Sherman, and G. Kurizki, Phys. Rev. A **50**, 5301 (1994).
[10] T. Ojanen and J. Salo, arXiv:cond-mat/0603709 (unpublished).
[11] L. D. Landau and E. M. Lifshitz, *Mechanics* (Pergamon, Oxford, 1976).
[12] Yu. Makhlin, G. Schön, and A. Shnirman, Rev. Mod. Phys. **73**, 357 (1999).
[13] R. Schoelkopf, A. Clerk, S. Girvin, K. Lehnert, and M. Devoret, in *Quantum Noise in Mesoscopic Physics*, edited by Yu. V. Nazarov, NATO Science Series II Vol. 97 (Kluwer, Dordrecht, 2003).
[14] H. J. Carmichael, *Statistical Methods in Quantum Optics 1: Master Equations and Fokker-Planck Equations* (Springer, Berlin, 1999).
[15] T. P. Orlando, J. E. Mooij, L. Tian, C. H. van der Wal, L. Levitov, S. Lloyd, and J. J. Mazo, Phys. Rev. B **60**, 15398 (1999).
[16] V. B. Braginsky and F. Ya. Khalili, *Quantum Measurement* (Cambridge University Press, Cambridge, 1992).